

A FINITE RATE OF INNOVATION MULTICHANNEL SAMPLING HARDWARE SYSTEM FOR MULTI-PULSE SIGNALS

Ning Fu, Member, IEEE, Liwen Sun, Guoxing Huang, Shuaile Du

Dept. of Automatic Test and Control, Harbin Institute of Technology
Harbin, 150080, Heilongjiang Province, P.R.China
Email: funinghit_paper@163.com

ABSTRACT

Multi-pulse signals are composed of finite pulse streams of arbitrary pulse shape. With the pulse shape known, a multi-channel sampling scheme for multi-pulse signals can operate at the rate of innovation, which is much lower than the Nyquist rate. The sampling system is based on low-pass filters, oscillators and integrators. By now there is no hardware to practice the approach. In this paper, we design a hardware system and discover that the non-idealities of low-pass filters will lead to failing in signal reconstruction. We research how the low-pass filters affect the reconstruction and solve the problem by channel calibration. The experiments show that channel calibration compensates most of the errors induced by low-pass filters, and this approach can achieve better estimation of time-delays and amplitudes of multi-pulse signals with a known pulse shape.

Index Terms— Finite rate of innovation, sub-Nyquist sampling, multi-pulse reconstruction, hardware system

1. INTRODUCTION

In modern signal processing, analog signals must be transmitted into digital signals by sampling. To perfectly reconstruct the original signal from its samples, the Shannon-Nyquist theorem requires the sampling rate to be twice as its highest frequency, i.e., the Nyquist rate. However, the Nyquist rate of wideband signals is too high to achieve [1-3].

To reduce the sampling rate, Vetteri *et al* exploit a new sampling theorem for signals with finite rate of innovation (FRI). FRI signals have a finite number of degrees of freedom per unit time [4-6]. The minimal sampling rate for a FRI signal is equal to its innovation rate, which is usually much lower than its Nyquist rate.

As a representative of typical FRI signals, the multi-pulse signal is composed of several pulses in a short time. When the pulse shape is known, each pulse of the multi-pulse signal is specified by its time-delay and amplitude. Multi-pulse signals are widely used in neuronal activity [7],

bio-imaging [8] and ultrawideband communications [9-10]. Since the multi-pulse signal is highly compact in time, its Nyquist rate is much higher than its innovation rate. But considering its parametric characteristic, it can be sampled by FRI sampling schemes at a much lower rate and reconstructed by special algorithms.

The FRI sampling schemes of multi-pulse signals can be divided into single-channel and multichannel sampling schemes. For single-channel cases, the multi-pulse signal is sampled by designed sampling kernels. Kernels which have infinite support in time cannot be achieved physically, such as sinc and Gaussian sampling kernels [4]. In contrast, polynomial reproducing kernels, exponential reproducing kernels, rational kernels [11] and the SoS (Sum of Sincs) [8] kernel are highly compact in time.

Compared with the single-channel cases, the multichannel sampling scheme reduces the sampling rate and the complication to design sampling kernel in each channel. A multichannel system comprised of two first-order resistor-capacitor networks is put forward in [12]. Another multichannel system based on E-spline kernels is proposed for pulses of arbitrary shape [13]. There are other two alternative multichannel schemes for pulses of arbitrary shape. One is based on a union of subspaces [14], and the other one is based on filter banks to sample radar pulse signals [15-16].

Up to now, most sampling schemes for multi-pulse signals have too many restrictions to be achieved physically. Based on the ideas of Xampling, i.e., sampling for structured analog signals [17-19], Eldar *et al* propose a multichannel sampling scheme similar to the modulated wideband converter (MWC) [17, 20-21] system to sample pulse streams at the rate of innovation [22]. They discuss the cases of sampling finite and infinite pulse streams and propose pulse sequence modulation as an alternative approach.

In this paper, based on the works of Eldar *et al* [22], we design a multichannel sampling hardware system using pulse sequence modulation, and verify that it can achieve the rate of innovation of multi-pulse signals. In addition, when testing the performance of the system, we find that the non-idealities of low-pass filters will lead to failing in signal reconstruction. So we propose an approach to calibrate each channel and compensate the estimation errors induced by filters. The hardware experiments demonstrate that, the sig-

This work was supported by National Natural Science Foundation of China (NSFC, No. 61102148 and No. 61671177).

nal reconstruction is more precise after channel calibration. Besides, multi-pulse signals can be recovered from the proposed minimal-rate samples.

The remainder of this paper is organized as follows. In Part 2 we introduce the multichannel sampling scheme for multi-pulse signals with pulse sequence modulation. In Part 3 we design a hardware system, discuss the non-idealities of low-pass filters and the approach of channel calibration. Part 4 lists the hardware experiments and results. Finally we draw conclusions in Part 5.

2. SAMPLING AND RECONSTRUCTION OF MULTI-PULSE SIGNALS

2.1. Model of Multi-pulse Signals

The multi-pulse signal $x(t)$ shown in **Fig. 1** contains L pulses of a known pulse shape $h(t)$ in the time-window $[0, T)$ [18]. We assume that in $[0, T)$, none of the L pulses is interceptive. $x(t)$ can be defined as

$$x(t) = \sum_{l=1}^L a_l h(t - t_l), t_l \in [0, T). \quad (1)$$

From (1), in $[0, T)$, $x(t)$ has $2L$ degrees of freedom, $\{t_l, a_l\}_{l=1}^L$. So the rate of innovation of $x(t)$ is $2L/T$.

$X[k]$ is the Fourier series coefficients of $x(t)$. $H(\omega)$ is the CTFT of $h(t)$. The relation between $X[k]$ and $\{t_l, a_l\}_{l=1}^L$ can be expressed as [8]

$$X[k] = \frac{1}{T} H\left(\frac{2\pi}{T}k\right) \sum_{l=1}^L a_l e^{-j\frac{2\pi}{T}kt_l}, k \in \mathbb{k}. \quad (2)$$

\mathbb{k} denotes a set of K consecutive integers for which $H(2\pi k/T) \neq 0, \forall k \in \mathbb{k}$. \mathbf{H} denotes a $K \times K$ diagonal matrix with k th diagonal element $(1/T)H(2\pi k/T)$. And $\mathbf{V}(\mathbf{t})$ denotes a $K \times L$ matrix with kl th element $e^{-j\frac{2\pi}{T}kt_l}$, where $\mathbf{t} = \{t_1, \dots, t_L\}$. \mathbf{a} denotes a length- L vector with l th element a_l . \mathbf{x} denotes a length- K vector with k th element $X[k]$. Then (2) can be written in a matrix form as [22]

$$\mathbf{x} = \mathbf{H}\mathbf{V}(\mathbf{t})\mathbf{a}. \quad (3)$$

(3) depicts the reconstruction model of multi-pulse signals. If the Fourier series coefficients $X[k]$ are known, $\{t_l\}_{l=1}^L$ can be estimated by the annihilating filter [1]. Other algorithms such as matrix-pencil [23] and ESPRIT [24] are also applicable. Then $\{a_l\}_{l=1}^L$ can be estimated as

$$\mathbf{a} = \mathbf{V}^\dagger(\mathbf{t})\mathbf{H}^{-1}\mathbf{x}. \quad (4)$$

2.2. Multichannel Sampling Scheme

The multichannel sampling scheme obtains $\{c_i\}_{i=1}^p$ as the mixing Fourier series coefficients of $x(t)$. The scheme is comprised of low-pass filters, mixers and integrators. As depicted in **Fig. 2**, in the i th channel, $x(t)$ is modulated by $s_i(t)$. Then the output signal of the mixer is integrated over

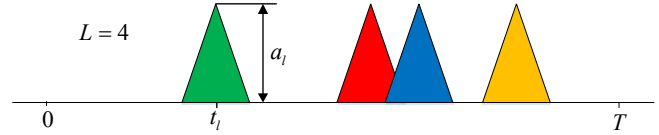


Fig. 1. Example of a multi-pulse signal with $L = 4$ pulses. In this example, two of the pulses are overlapping.

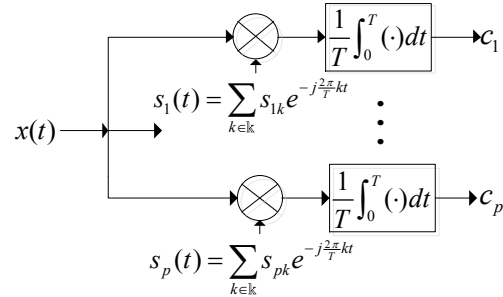


Fig. 2. Multichannel sampling scheme of multi-pulse signals

the window $[0, T)$. $s_i(t)$ is described as [22]

$$s_i(t) = \sum_{k \in \mathbb{k}} s_{ik} e^{-j\frac{2\pi}{T}kt}, i = 1, \dots, p. \quad (5)$$

\mathbf{S} denotes a $p \times L$ matrix with ik th element s_{ik} . \mathbf{c} denotes a length- p vector with i th element c_i . Then a matrix form is obtained as

$$\mathbf{c} = \mathbf{S}\mathbf{x}. \quad (6)$$

Then $X[k]$ can be recovered as follows:

$$\mathbf{x} = \mathbf{S}^\dagger \mathbf{c} \quad (7)$$

The symbol \dagger represents left-inverse of a matrix. Considering that the modulating matrix \mathbf{S} should have full column rank, the condition $p \geq K \geq 2L$ is necessary [22]. Since there are p samples obtained in $[0, T)$, the sampling rate is $\rho = p/T$. When $p = K = 2L$, $\rho_{min} = 2L/T$, so this scheme can operate at the rate of innovation.

2.3. Pulse Sequence Modulation

Design of $s_i(t)$ in (5) is complicated. Now consider using pulse sequences $\{r_i(t)\}_{i=1}^p$ instead. In order to remove the frequency components contained in $\{r_i(t)\}_{i=1}^p$ but not specified by \mathbb{k} , low-pass filters are needed before modulation.

$r_i(t) (i = 1, \dots, p)$ is given as

$$r_i(t) = \sum_{m \in \mathbb{Z}} \sum_{n=0}^{N-1} \alpha_i[n] r\left(t - \frac{n}{N}T - mT\right). \quad (8)$$

In (8), $r(t)$ is a single rectangular pulse defined as

$$r(t) = \begin{cases} 1 & t \in \left[0, \frac{T}{N}\right] \\ 0 & t \notin \left[0, \frac{T}{N}\right] \end{cases} \quad (9)$$

We choose $\alpha_i[n]$ as sequences of ± 1 , which are equal to cyclic shifts of one basic sequence. The basic sequence is composed by ± 1 randomly [22].

In the i th channel, let $r_i(t)$ be the input signal of the low-pass filter and $\tilde{r}_i(t)$ denotes the output signal. It can be expressed as

$$\tilde{r}_i(t) = s_{ik} e^{j\frac{2\pi}{T}kt}, k \in \mathbb{K}, i = 1, \dots, p. \quad (10)$$

To make sure $\tilde{r}_i(t)$ is real valued, \mathbb{K} should satisfy (11). That means K is an odd number and $p \geq K \geq 2L + 1$.

$$\mathbb{K} = -\left\lfloor \frac{K}{2} \right\rfloor, \dots, 0, \dots, \left\lfloor \frac{K}{2} \right\rfloor \quad (11)$$

$R(\omega)$ is the CTFT of $r(t)$. Denote by $g(t)$ the frequency response of the low-pass filters. $G(\omega)$ is the CTFT of $g(t)$. Then s_{ik} in (5) can be determined by (12).

$$s_{ik} = \frac{1}{T} \sum_{n=0}^{N-1} \alpha_i[n] R\left(\frac{2\pi}{T}k'\right) G\left(\frac{2\pi}{T}k'\right) e^{-j\frac{2\pi}{N}k'n} \quad (12)$$

In (12), $i = 1, \dots, p$ and $k' = -k, k \in \mathbb{K}$. Then (12) can be written in a matrix form as

$$\mathbf{S} = \mathbf{A}\mathbf{W}\mathbf{\Phi}. \quad (13)$$

In (13), \mathbf{A} denotes a $p \times N$ matrix with in th element $\alpha_i[n]$. It must have full column rank. \mathbf{W} denotes a $N \times K$ matrix with nk th element $e^{-j\frac{2\pi}{N}k'n}$. $\mathbf{\Phi}$ denotes a $p \times K$ matrix with ik th element defined as

$$\phi_{ik} = \frac{1}{T} R\left(\frac{2\pi}{T}k'\right) G\left(\frac{2\pi}{T}k'\right). \quad (14)$$

3. HARDWARE SYSTEM DESIGN AND ANALYSIS

3.1. Hardware Design

Our hardware is designed to sample multi-pulse signals composed of 2 pulses. The highest frequency of the multi-pulse signal is less than 5 kHz. There are five sampling channels in our hardware system. And we use the annihilating filter to recover time-delays of the Gaussian pulses.

The structure of each channel in our hardware system is shown in Fig. 3. Each channel is comprised of MAX274 (low-pass filter), AD633 (analog multiplier) and a first-order RC network as integrator. The whole hardware system works on a PXI platform. PXIe-5442 generates multi-pulse signals. PXIe-6368 and PXI-6255 are multifunctional data acquisition devices developed by National Instruments (NI). They also play a role of generating modulating pulse sequences input to the five channels. The chassis PXIe-1082 offers trigger bus for synchronization in the five channels.

MAX274 is an eighth-order continuous-time active power filter. It contains four independent cascadable second-order sections. Each section can implement the filter response of Butter-worth, Bessel or Chebyshev only by four external resistors. Based on MAX274, we design a sixth-order Cheybeshev Type I low-pass filter with the cut-off frequency higher than 400Hz. It is required to have a decay

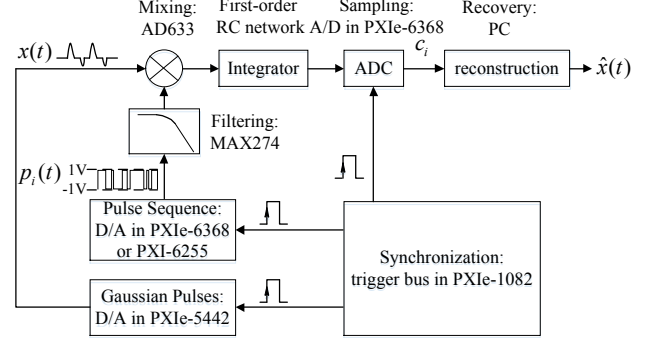


Fig. 3. Hardware structure of each sampling channel

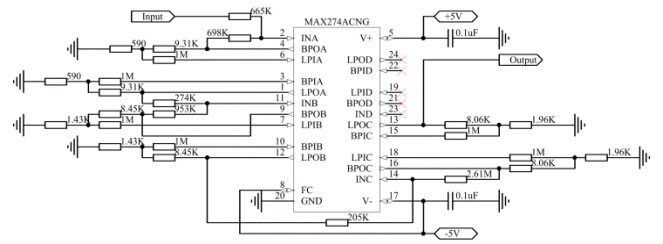


Fig. 4. Circuit of designed low-pass filter by MAX274

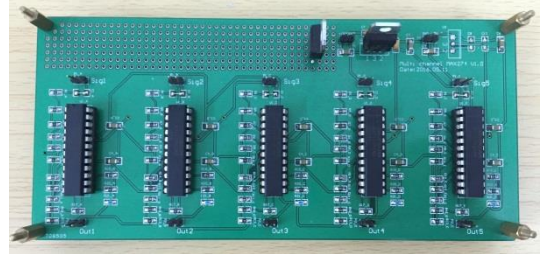


Fig. 5. Real product of low-pass filters in 5 channels

of -20dB at 600Hz. The peripheral circuit of MAX274 is shown in Fig. 4, and the real product is shown in Fig. 5.

3.2. Non-idealities of Low-pass Filters

Considering the non-idealities of low-pass filters, that is, $\{G_i(\omega)\}_{i=1}^p$ of low-pass filters in p channels are hard to be ideal or identical, and the output of low-pass filters may contain DC bias. So (13) can be updated as

$$\tilde{\mathbf{S}} = (\mathbf{A}\mathbf{W}) \odot \tilde{\mathbf{\Phi}} + \mathbf{B}. \quad (15)$$

\odot denotes point multiplication of two matrixes. In (13) and (15), the only difference between $\mathbf{\Phi}$ and $\tilde{\mathbf{\Phi}}$ is that, for the element of $\tilde{\mathbf{\Phi}}$, $G\left(\frac{2\pi}{T}k'\right)$ is changed into $G_i\left(\frac{2\pi}{T}k'\right)$. Let $m = \left\lfloor \frac{K}{2} \right\rfloor + 1$. Then \mathbf{B} denotes a $p \times K$ matrix with the m th column defined as the DC bias induced by low-pass filters in each channel, and the other columns are all zero vectors.

In conclusion, the non-idealities of low-pass filters affect the modulating matrix \mathbf{S} . According to (15), if the actual

frequency response is obtained by measurement, each channel can be calibrated by correcting the matrix \mathbf{S} . After channel calibration, the original multi-pulse signals will be recovered from samples more precisely. An alternative method of channel calibration is proposed in the next section.

3.3. Channel Calibration

The key of channel calibration is to obtain the actual frequency responses of low-pass filters in each channel. The specific steps of our proposed method are listed as follows:

Step 1, Generation of input signals. Generate sinusoidal signals with different frequencies $f_k = k/T, k = 0, \dots, \lfloor \frac{K}{2} \rfloor$ and input them to the low-pass filters successively. The amplitudes are set to 1V and the initial phases are set to 0.

Step 2, Measurement of output signals. In the i th channel, when the frequency of the input sinusoidal signal is $f_k = k/T$, measure the amplitudes $A_i(k)$ and phases $\varphi_i(k)$ of the output signals.

Step 3, Calculating frequency responses. In the i th channel, the frequency response $G_i(k)$ of the low-pass filter at $f_k = k/T$ can be calculated as (16). For the negative frequencies $f_{\tilde{k}} = \tilde{k}/T, \tilde{k} = -\lfloor \frac{K}{2} \rfloor, \dots, 0$ specified by \mathbb{k} , the frequency responses are conjugated with $G_i(k), k = 0, \dots, \lfloor \frac{K}{2} \rfloor$.

$$G_i(k) = A_i(k)e^{\varphi_i(k)} \quad (16)$$

Step 4, Measurement of DC bias. Let the input of the low-pass filter in each channel to be grounded, and the measured output voltage is the value of DC bias.

Step 5, Correction of the modulating matrix. Correct the modulating matrix \mathbf{S} using the actual frequency responses $\{G_i(k)\}_{i=1}^p$ of the low-pass filters as (15).

Step 6, Recovering Fourier series coefficients. Use the corrected modulating matrix \mathbf{S} to recover the correct Fourier series coefficients of multi-pulse signals as (7).

4. HARDWARE EXPERIMENTS

We assume the pulse shape is Gaussian and $x(t)$ is formulated as follows:

$$x(t) = \sum_{l=1}^L a_l e^{-\frac{(t-t_l)^2}{2\sigma^2}} \quad (17)$$

Let $L = 2, \sigma = 2 \times 10^{-4}, T = 5 \times 10^{-3}$ s. Since $p = 5$, our hardware system require 5 samples at least. Denote by $\{\tilde{t}_l\}_{l=1}^L$ the recovered time-delays and $\{\tilde{a}_l\}_{l=1}^L$ the recovered amplitudes of multi-pulse signals. The evaluation indicators of reconstruction results are listed as follows [8]:

$$t_{l_{MSE}} = \frac{1}{L} \sum_{l=1}^L (\tilde{t}_l - t_l)^2 \quad (18)$$

$$a_{l_{MSE}} = \frac{1}{L} \sum_{l=1}^L (\tilde{a}_l - a_l)^2 \quad (19)$$

According to (18) and (19), with the value of $t_{l_{MSE}}$ or $a_{l_{MSE}}$ smaller, the reconstruction is more precise. We change the values of $\{t_l, a_l\}_{l=1}^L$ and obtain three groups of hardware experiment results, shown in **Tab. 1** and **Tab. 2**.

4.1. Before Channel Calibration

Tab. 1 shows the estimated time-delays and amplitudes and the evaluation results of signal reconstruction before channel calibration. The data proves that, without channel calibration, the non-idealities of low-pass filters lead to failing in signal reconstruction.

Tab. 1. Experiment results before channel calibration

No.	$\{t_l, a_l\}_{l=1}^L$	$\{\tilde{t}_l, \tilde{a}_l\}_{l=1}^L$	$t_{l_{MSE}}/T^2$	$a_{l_{MSE}}$
1	{0.3T, 0.3}	{0.363T, 1.292}	2.500E-5	6.138E-1
	{0.7T, 0.8}	{0.363T, 1.292}		
2	{0.2T, 0.4}	{0.984T, 9.190E+13}	3.810E-1	8.446E+27
	{0.6T, 0.8}	{0.984T, -9.190E+13}		
3	{0.5T, 0.7}	{0.045T, 2.558E+15}	3.887E-1	6.542E+30
	{0.8T, 0.3}	{0.045T, -2.558E+15}		

4.2. After Channel Calibration

After channel calibration, the experiment results are shown in **Tab. 2**. We can conclude that the approach channel calibration improves the precision of signal reconstruction.

Tab. 2. Experiment results after channel calibration

No.	$\{t_l, a_l\}_{l=1}^L$	$\{\tilde{t}_l, \tilde{a}_l\}_{l=1}^L$	$t_{l_{MSE}}/T^2$	$a_{l_{MSE}}$
1	{0.3T, 0.3}	{0.292T, 0.218}	3.464E-5	6.019E-3
	{0.7T, 0.8}	{0.703T, 0.729}		
2	{0.2T, 0.4}	{0.023T, 0.407}	1.685E-2	2.297E-3
	{0.6T, 0.8}	{0.552T, 0.733}		
3	{0.5T, 0.7}	{0.509T, 0.699}	5.468E-3	6.978E-4
	{0.8T, 0.3}	{0.904T, 0.337}		

5. CONCLUSIONS

In this paper, based on the work by Eldar *et al* [22], a multi-channel sampling hardware system is designed to sample multi-pulse signals at the rate of innovation. The hardware experiments verify that this approach can acquire better estimation of time-delays and amplitudes of multi-pulse signals from the proposed minimal-rate samples. In addition, the non-idealities of low-pass filters in the hardware system will lead to failing in signal reconstruction. With channel calibration, i.e., obtaining the actual frequency responses of the filters and correcting the modulating matrix, the signal reconstruction will be more precise.

6. REFERENCES

- [1] H. Nyquist, "Certain topics in telegraph transmission theory," *Proceedings of the IEEE*, vol. 90, no. 2, pp. 280-305, 2002.
- [2] M. Unser, "Sampling—50 Years after Shannon," *Proceedings of the IEEE*, vol. 88, no. 4, pp. 569-587, 2000.
- [3] S. Nagesh and C. S. Seelamantula, "FRI sampling and reconstruction of asymmetric pulses," *IEEE Intl. Conf. on Acoust., Speech and Signal Process. (ICASSP)*, pp. 5957-5961, 2015.
- [4] M. Vetterli, P. Marziliano, and T. Blu, "Sampling signals with finite rate of innovation," *IEEE Trans. Signal Process.*, vol. 50, no. 6, pp. 1417-1428, 2002.
- [5] T. Blu, P. L. Dragotti, M. Vetterli, P. Marziliano, and L. Coulot, "Sparse sampling of signal innovations," *IEEE Signal Process. Mag.*, vol. 25, no. 2, pp. 31-40, 2008.
- [6] M. Vetterli, P. Marziliano, and T. Blu, "Sampling discrete-time piecewise bandlimited signals," *Proc. Sampling Theory and Applications Workshop*, pp. 97-102, 2001.
- [7] J. Onativia and P. L. Dragotti, "Sparse sampling: theory, methods and an application in neuroscience," *Biological Cybernetics*, vol. 109, no. 1, pp. 125-139, 2015.
- [8] R. Tur, Y. C. Eldar, and Z. Friedman, "Innovation rate sampling of pulse streams with application to ultrasound imaging," *IEEE Trans. Signal Process.*, vol. 59, no. 4, pp. 1827-1842, 2011.
- [9] M. Greitans and R. Shavelis, "Reconstruction of sequences of arbitrary shaped pulses from its low pass or band pass approximations using spectrum extrapolation," *Eur. Signal Process. Conf. (EUSIPCO)*, pp. 1607-1611, 2010.
- [10] A. M. Pistea, I. Nicolaescu, E. Radoi and L. Tuta, "Parametric estimation of UWB signals with sub-Nyquist sampling," *International Symposium on Signals, Circuits and Systems (ISSCS)*, pp. 1-4, 2015.
- [11] P. L. Dragotti, M. Vetterli, and T. Blu, "Sampling moments and reconstructing signals of finite rate of innovation: Shannon meets Strang-Fix," *IEEE Trans. Signal Process.*, vol. 55, no. 5, pp. 1741-1757, 2007.
- [12] C. Seelamantula and M. Unser, "A generalized sampling method for finite-rate-of-innovation-signal reconstruction," *IEEE Signal Process. Lett.*, vol. 15, pp. 813-816, 2008.
- [13] H. A. Asl, P. L. Dragotti, and L. Baboulaz, "Multichannel sampling of signals with finite rate of innovation," *IEEE Signal Process. Lett.*, vol. 17, no. 8, pp. 762-765, 2010.
- [14] K. Gedalyahu and Y. C. Eldar, "Time delay estimation from low rate samples: A union of subspaces approach," *IEEE Trans. Signal Process.*, vol. 58, no. 6, pp. 3017-3031, 2010.
- [15] G. Itzhak, E. Baransky, N. Wagner, I. Shmuel, E. Shoshan, and Y. C. Eldar, "A hardware prototype for sub-Nyquist radar sensing," *Proc. 2013 ITG Int. Conf. Systems, Communication and Coding (SCC)*, pp. 1-6, 2013.
- [16] E. Baransky, G. Itzhak, N. Wagner, I. Shmuel, E. Shoshan, and Y. C. Eldar, "Sub-Nyquist radar prototype: Hardware and algorithm," *IEEE Trans. Aerosp. Electron. Syst.*, vol. 50, no. 2, pp. 809-822, 2014.
- [17] M. Mishali, Y. C. Eldar, O. Dounaevsky, and E. Shoshan, "Xampling: Analog to digital at sub-Nyquist rates," *IET Circuits Devices Syst.*, vol. 5, no. 1, pp. 8-20, 2011.
- [18] E. Matusiak and Y. C. Eldar, "Sub-Nyquist sampling of short pulses," *IEEE Trans. Signal Process.*, vol. 60, no. 3, pp. 1134-1148, 2012.
- [19] M. Mishali, Y. C. Eldar, and A. Elron, "Xampling: Signal acquisition and processing in union of subspaces," *IEEE Trans. on Signal Process.*, vol. 59, no. 10, pp. 4719-4734, 2011.
- [20] M. Mishali and Y. C. Eldar, "Blind multiband signal reconstruction: Compressed sensing for analog signals," *IEEE Trans. Signal Process.*, vol. 57, no.3, pp. 993-1009, 2009.
- [21] M. Mishali and Y. C. Eldar, "From theory to practice: Sub-Nyquist sampling of sparse wideband analog signals," *IEEE J. Sel. Topics Signal Process.*, vol. 4, no. 2, pp. 375-391, 2010.
- [22] K. Gedalyahu, R. Tur, and Y. C. Eldar, "Multichannel sampling of pulse streams at the rate of innovation," *IEEE Trans. Signal Process.*, vol. 59, no. 4, pp. 1491-1504, 2011.
- [23] Y. Hua and T. K. Sarkar, "Matrix pencil method for estimating parameters of exponentially damped/undamped sinusoids in noise," *IEEE Trans. Acoust., Speech, Signal Process.*, vol. 38, no. 5, pp. 814-824, 1990.
- [24] R. Roy and T. Kailath, "ESPRIT—Estimation of signal parameters via rotational invariance techniques," *IEEE Trans. Acoust., Speech, Signal Process.*, vol. 37, no. 7, pp. 984-995, 1989.